Structural and magnetic properties of Co-doped (La,Sr)TiO_3 epitaxial thin films probed using x-ray magnetic circular dichroism

2009 J. Phys.: Condens. Matter 21 406001

(http://iopscience.iop.org/0953-8984/21/40/406001)

J. Phys.: Condens. Matter **21** (2009) 406001 (6pp) doi:10.1088/0953-8984/21/40/406001

Structural and magnetic properties of Co-doped (La, Sr)TiO_3 epitaxial thin films probed using x-ray magnetic circular dichroism

O Copie[1], K Rode[2], R Mattana[1], M Bibes[1], V Cros[1], G Herranz[1,5], A Anane[1], R Ranchal[1,6], E Jacquet[1], K Bouzehouane[1], M-A Arrio[3], P Bencok[4,7], N B Brookes[4], F Petroff[1] and A Barthélémy[1]

[1] Unité Mixte de Physique CNRS/Thales, Campus de l'Ecole Polytechnique, 1 Avenue A Fresnel, 91767 Palaiseau, France and Université Paris-Sud 11, 91405 Orsay, France
[2] Center for Research on Adaptative Nanostructures and Nanodevices, Trinity College Dublin, Dublin 2, Republic of Ireland
[3] Institut de Minéralogie et de Physique des Milieux Condensés CNRS, Université Pierre et Marie Curie, 140 rue de Lourmel 75015 Paris, France
[4] European Synchrotron Radiation Facility, 6 rue Horowitz, 38083 Grenoble, France

E-mail: agnes.barthelemy@thalesgroup.com

Received 23 April 2009, in final form 6 July 2009
Published 8 September 2009
Online at stacks.iop.org/JPhysCM/21/406001

Abstract

We report a study of Co-doped $La_{0.37}Sr_{0.63}TiO_{3-\delta}$ thin films grown by pulsed laser deposition in various oxygen pressure conditions. X-ray absorption spectroscopy and magnetic circular dichroism measurements at the Co $L_{2,3}$ edges reveal that the cobalt mainly substitutes for the titanium and is in an ionic state. Nevertheless, in some films, indications of additional cobalt metallic impurities were found, suggesting that the intrinsic character of this magnetic system remains questionable.

(Some figures in this article are in colour only in the electronic version)

An approach in spintronics [1] is to design sources of spin-polarized current by doping semiconductors with magnetic ions. Dilute magnetic materials based on III–V semiconductors have already demonstrated the potential of this approach [2]. Regarding applications, the Curie temperature of III–V ferromagnetic semiconductors is still below room temperature. Since the discovery of room temperature (RT) ferromagnetism in Co-doped TiO_2 [3] and the prediction of RT ferromagnetism in Co-doped ZnO [4], an intense research has emerged on other diluted magnetic oxides. However, reports in this field are controversial and an intense theoretical and experimental debate concerns the intrinsic or Co cluster-based origin of the magnetism. A typical example is that of Co-doped ZnO [5, 6].

Most diluted magnetic systems are designed by the magnetic doping of a semiconducting host. Following the observation of RT ferromagnetism in (La, Sr)TiO_3 doped with 2% of Co (Co–LSTO) [7], we have considered this alternative approach based on a strongly correlated metal host [8]. In a previous work, we reported an extensive chemical and structural characterization that did not evidence Co segregation [9]. We also inferred a finite spin polarization for Co-doped (La, Sr)TiO_3 since a tunnel magnetoresistance of 20% was measured in Co-LSTO/$LaAlO_3$/Co junctions [9]. More recently, the presence of Co clusters, revealed by high-

[5] Present address: Institut de Ciència de Materials de Barcelona, CSIC, Campus de la UAB, 08193 Bellaterra, Cataluyna, Spain.
[6] Present address: Departamento Fisica de Materiales, Facultad de Ciencias Fisicas, Universidad Complutense de Madrid, Ciudad Universitaria s/n, Madrid 28040, Spain.
[7] Present address: Diamond Light Source Ltd, Didcot OX11 0DE, Oxford, UK.

resolution transmission electron microscopy (HRTEM), in (La, Sr)TiO_3 doped with 5% of Co was reported by Zhang *et al* [10] suggesting an extrinsic mechanism for ferromagnetism.

The magnetic signal of a diluted magnetic system is in general very small and close to the sensitivity of most standard magnetometry techniques. For very low doping levels, the dopants may even be impossible to detect with conventional chemical and structural characterization equipments. Then, x-ray absorption (XAS) and x-ray magnetic circular dichroism (XMCD) appear as powerful and more appropriate techniques for the study of diluted magnetic systems due to their elemental selectivity and great sensitivity.

In this paper we report the structural and magnetic properties of Co–LSTO thin films grown under different pressure conditions. We have used XAS and XMCD to study the local order and the ionic state of Co in the LSTO host and to probe selectively the magnetic contribution of the different elements. Co–LSTO epitaxial thin films were grown by pulsed laser deposition (PLD) using a frequency tripled ($\lambda = 355$ nm) Nd:yttrium aluminum garnet (YAG) laser, on $SrTiO_3$(001) (STO) substrates. The target was prepared by a standard solid-state reaction and had a nominal composition of $La_{0.37}Sr_{0.63}Ti_{0.98}Co_{0.02}O_3$. The growth was carried out with a laser repetition rate of 5 Hz and an energy density of 2.8 J cm^{-2}. The films were grown in a range of oxygen pressure between 10^{-4} and 10^{-7} mbar while maintaining the substrate temperature at 700 °C. High-resolution four-circle x-ray diffraction was used for the structural characterization of the samples. Symmetric 2θ–ω scans were used to determine the out-of-plane lattice parameter of the film. θ–2θ/ω area scans were collected close to the (013) reflections and were plotted in reciprocal space. XAS and XMCD measurements, at the O K edge and the Co $L_{2,3}$ edges, were performed at the European synchrotron radiation facility (ESRF) in Grenoble, beamline ID08, in a temperature range from 10 to 300 K with a magnetic field up to 3 T. XAS and XMCD spectra at Co $L_{2,3}$ edges ($2p \rightarrow 3d$ transitions) were recorded in total electron yield mode (TEY) with the photon wavevector and the applied magnetic field perpendicular to the sample surface or with an angle of 20° between the magnetic field and the sample surface. XAS and XMCD techniques are surface sensitive due to the low escape depth of the photoelectrons (≈3–4 nm).

In figure 1(a), we show high-angle x-ray diffraction 2θ–ω spectra for films grown at different oxygen pressures. No evidence of parasitic phases or Co clusters is found, consistent with a previous extensive structural study [9]. The values of the full width at half maximum (FWHM) of the rocking curve of the (003) reflection was $\Delta\omega_{003} \approx 0.18°$. These data and the results from ϕ-scans indicate an epitaxial growth for all pressure conditions. The evolution of the (003) diffraction peak and the extracted out-of-plane parameter of the Co–LSTO films as a function of the oxygen growth pressure are shown respectively in figures 1(b) and (c). A large increase of the c-axis lattice parameter as the growth pressure decreases is observed in good agreement with the expected creation of oxygen vacancies. Reciprocal space maps close to the (013) reflection of Co–LSTO are shown on figures 1(d) and (e) respectively for samples grown at 10^{-4} and 10^{-7} mbar. They clearly indicate that in both cases, the films are fully strained since the reflections from the substrates and the film are on the same line. The c/a ratio is larger for the sample grown at the lowest oxygen pressure ($c/a = 1.01$ and 1.02 was respectively measured for 10^{-4} and 10^{-7} mbar). From these structural considerations, we can assume that the incorporation of oxygen vacancies at low pressure in our sample results in an elongation of the cell along the c-axis.

For XAS and XMCD experiments at the Co $L_{2,3}$ edges and O K edge, two 50 nm thick samples at both extremes of the oxygen growth pressure range (10^{-7} and 10^{-4} mbar) and one 150 nm thick sample grown at 10^{-6} mbar were selected. XAS and XMCD experiments were also performed at the Ti $L_{2,3}$ edges but no XMCD signal was measured and therefore they will not be discussed in the following.

In figure 2, we show XAS spectra at O K edge, recorded at $T = 10$ K, for 50 nm thick films grown at 10^{-7} mbar and 10^{-4} mbar respectively. The first peak at ∼530 eV corresponds to the transition between the O 1s orbitals and O 2p orbitals hybridized with Ti 3d t_{2g} orbitals [11] (other features, at higher energies, are related to a Sr 4d–O 2p and La 5d–O 2p mix [11]). In our spectra, considering the peak at ∼530 eV, we can interpret the loss of intensity between high and low growth pressure in term of weaker hybridization between O 2p orbitals and the 3d orbitals [12] (i.e Co 3d and Ti 3d orbitals) in the films grown at low oxygen pressure. This is in good agreement with our XRD experiments, which show that the oxygen vacancies incorporation results in an elongation of the cell and thus the distance between the oxygen atoms and the first neighbors increases. No XMCD signal has been detected in both films.

In figure 3(a), we show Co $L_{2,3}$ edges spectra, recorded at $T = 10$ K, for 50 nm thick films grown at 10^{-7} mbar and 10^{-4} mbar respectively. We also show a typical $L_{2,3}$ edges spectrum for metallic cobalt in the inset of figure 3(a). Both spectra recorded for the Co–LSTO films exhibit fine structures at the Co $L_{2,3}$ edges characteristic of Co in an ionic state. Comparison with multiplet calculations [13] and experimental [14] spectra confirm the presence of Co^{2+} in octahedral symmetry as expected for Co^{2+} at Ti sites. This is particularly clear for the sample grown at higher pressure. Nevertheless, the low oxygen pressure case reveals a more complex behavior since the fine structure is less pronounced. Its weaker multiplet structure may be explained in term of a change in the crystal field splitting (10 Dq) as calculated by De Groot *et al* [13] when oxygen vacancies are introduced [15]. This change could be induced by a modification of the Co–O distance when the oxygen growth pressure is varied as proven by x-ray measurements (see figures 1(b) and (c)) and illustrated by the O K edge XAS spectra (see figure 2). When the oxygen growth pressure decreases the Co–O distance increases leading to a reduced Co 3d–O 2p overlap and consequently to a weaker 10 Dq and less well-defined features. Another origin of this weaker multiplet structure might be a more filled Co 3d shell due to the presence of oxygen vacancies-induced carriers related to the growth at low oxygen pressure. Consequently, the number of holes in the 3d shell is reduced resulting in a decreased intensity in the XAS spectrum. Lastly, this may also

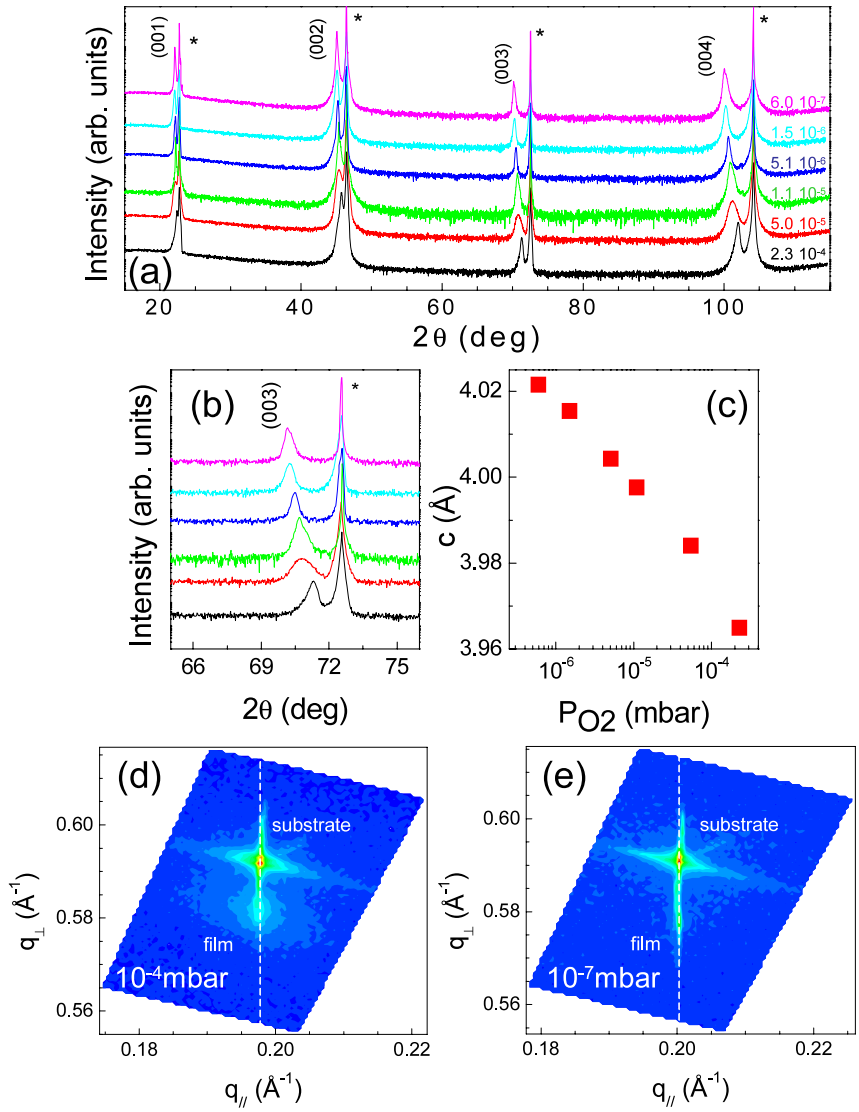

Figure 1. (a) High-angle x-ray diffraction 2θ–ω for films grown at different oxygen growth pressure (2.3×10^{-4}–6×10^{-7} mbar). The substrate diffraction peaks are denoted by a star and the corresponding thin film diffraction peak by (00l). (b) Evolution of the (003) diffraction peak as function of oxygen pressure. (c) Out of plane lattice parameter as a function of oxygen growth pressure. (d) and (e) Reciprocal space maps close to the (013) reflection of Co–LSTO films respectively for samples grown at 10^{-4} and 10^{-7} mbar.

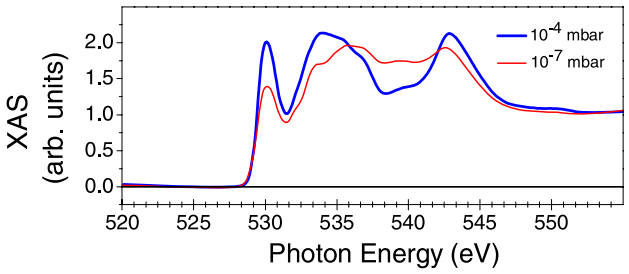

Figure 2. O K edge XAS spectra recorded in TEY mode at 10 K with an applied magnetic field of 3 T perpendicular to the sample plane, for films grown at 10^{-7} (red) and 10^{-4} (blue). The spectra have been normalized for comparison.

reflect the presence of an additional Co-rich parasitic phase which induces an average of the ensemble of Co atoms in the metallic clusters and the Co ions at the Ti sites.

The XMCD spectra are shown in figure 3(b) and reveal some relevant differences between the two samples. For the sample grown at 10^{-4} mbar we see a well-defined fine structure in good agreement with a magnetism arising from cobalt in ionic state at high applied magnetic field. On the contrary, the spectrum for the sample grown at 10^{-7} mbar exhibits a weaker fine structure with only small shoulders at 777.7 and 779 eV and a shape closer to the one expected for metallic cobalt. Unfortunately, due to the low Co content (background contribution for isotropic spectra), it is difficult to calculate the orbital momentum (m_L) and the spin momentum (m_S) via the sum rules [16]. Nevertheless, from the dichroic signal, we can estimate the m_L/m_S ratio (background contribution is almost suppressed for XMCD spectra) which is 0.40 and 0.20 respectively for the sample grown at 10^{-4} mbar and 10^{-7} mbar.

To get a better insight into our XAS and XMCD spectra, we have calculated absorption spectra using an atomic

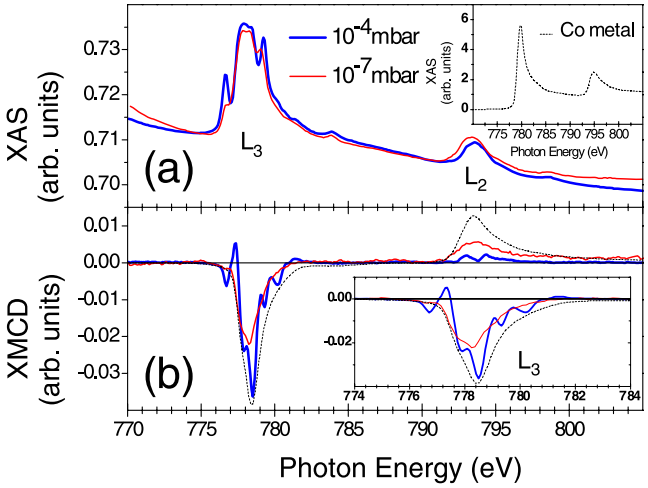

Figure 3. (a) Co $L_{2,3}$ edge XAS spectra recorded in TEY mode at 10 K with an applied magnetic field of 3 T perpendicular to the sample plane, for films grown at 10^{-7} (red) and 10^{-4} (blue) mbar. The inset shows a reference of metallic cobalt. (b) Co $L_{2,3}$ edge XMCD spectra recorded at 10 K with an applied magnetic field of 3 T perpendicular to the sample plane, for films grown at 10^{-7} (red) and 10^{-4} mbar (blue). The black curve is a reference of metallic cobalt.

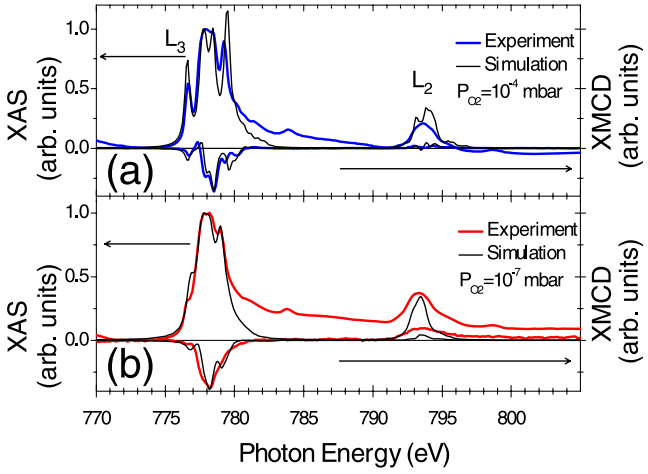

Figure 4. (a) XAS and XMCD experimental (blue) and simulated (black) spectra for the sample grown at 10^{-4} mbar. (b) XAS and XMCD experimental (red) and simulated (black) spectra for the sample grown at 10^{-7} mbar.

multiplet approach [17]. We state that the absorber is Co in a 2+ state in a crystal field with octahedral symmetry and with an applied magnetic field along the (001) direction. This leads to a C_{4h} final symmetry. An experimental value of 10 Dq on undoped $La_xSr_{1-x}TiO_3$ was found by resonant soft-x-ray emission spectroscopy (SXES) experiments by Higuchi *et al* [18, 19]. Considering this value of 10 Dq = 2.30 eV we calculate $\langle r^4_{3d1}\rangle$ for Ti^{3+} and $\langle r^4_{3d7}\rangle$ for Co^{2+} to adapt the crystal field splitting in our system using the code developed by Cowan [17]. We found 10 Dq = 1.21 eV. The simulated spectra yielding the best agreement were obtain at 10 K, for an exchange splitting of 0.01 eV and for $\kappa = 70\%$ (κ: Slater integral) in the high pressure case and $\kappa = 55\%$ in low pressure case. Such a decrease of κ is consistent with a reduction of the Co 3d–O 2p overlap [20] at low oxygen pressure.

In figures 4(a) and (b), we show experimental and simulated spectra for the high and low oxygen pressure case respectively. For the sample grown at 10^{-4} mbar (figure 4(a)), the simulated XAS and XMCD spectra, with 10 Dq = 1.21 eV, are in good agreement with the experimental data. Furthermore the values of the spin momentum ($m_S = 2.12\ \mu_B$) and the orbital momentum ($m_L = 0.87\ \mu_B$) extracted from the calculation give $m_L/m_S = 0.41$ which is close to the experimental value ($m_L/m_S = 0.40$). This is in good agreement with Co being in a 2+ state and substituting for Ti in the (La, Sr)TiO_3 matrix. For the sample grown at low oxygen pressure (figure 4(b)), the value of 10 Dq can be reduced due to larger La content or in our case to the possible presence of oxygen vacancies. For 10 Dq = 0.80 eV, leading to the best simulated spectra, the agreement between experimental and simulated XAS and XMCD spectra is less convincing. However, the intensity decrease of the features in the XAS spectrum due to the smaller crystal field parameter is quite well reproduced [13]. The persistence of a fine structure clearly establishes the presence of Co^{2+} in Ti site. The comparison between calculated and experimental values of m_L/m_S ratio reveals however a significant difference with the calculated m_L/m_S of 0.44 (with $m_S = 2.09\ \mu_B$ and $m_L = 0.93\ \mu_B$) against the experimentally observed ratio, $m_L/m_S = 0.20$. Such a discrepancy could be related to the presence of metallic Co clusters participating to the XMCD signal: an ionic phase with 2+ character and a metallic-like phase that contribute more to the magnetic signal at 3 T as revealed by the metal-like shape of the Co $L_{2,3}$ edge in XMCD spectra.

To obtain further information on the origin of magnetism in our films, we have performed hysteresis loop at the Co L_3 edge at $T = 10$ K for an applied magnetic field perpendicular to the sample surface and also at an angle of 20°. The results are presented in figure 5. We underline that this technique is only sensitive to the Co in the film avoiding any substrate contribution to the magnetic signal. For the sample grown at 10^{-4} mbar (figure 5(a)), the magnetization curve is characteristic of a paramagnetic behavior (without any anisotropy or hysteresis) with no evidence of saturation up to 3 T. This, together with results from XAS and XMCD suggest a paramagnetic behavior related to noncoupled Co in an ionic state substituting the Ti ions. For the sample grown at 10^{-7} mbar (figure 5(b)) as for the one grown at 10^{-6} mbar (not shown) one sees a small S-like shape as well as a clear anisotropy. This anisotropy may indicate a ferromagnetic behavior at the sample surface although no hysteresis is seen. However, it is very difficult to confirm it quantitatively due to the low Co content. It is also quite difficult to determine a magnetization value at zero field or a cycle aperture due to the low signal to noise ratio. This magnetic signal, together with the Co metallic-like XMCD spectrum, may suggest a nonnegligible contribution to the magnetic signal recorded at the Co L_3 edge arising from cobalt clusters in a metallic state.

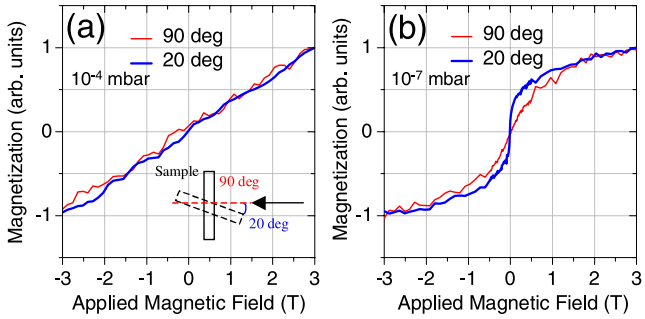

Figure 5. XMCD magnetization loop measured in TEY mode at Co L_3 edge for a high oxygen pressure film (a) and for a low oxygen pressure film (b) recorded for an angle between the applied magnetic field and the sample surface of 90° and 20° respectively. The applied magnetic field and the photon wavevector are both along the black arrow.

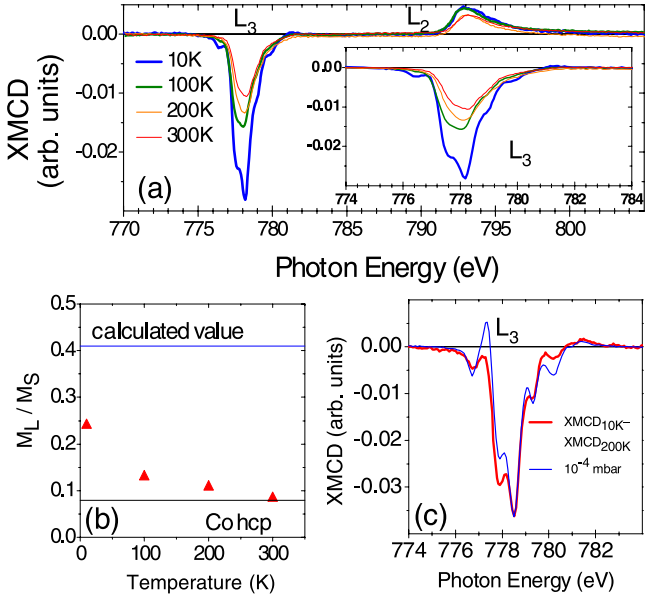

Figure 6. (a) XMCD spectra in TEY mode for a 150 nm thick sample grown at 10^{-6} mbar as a function of temperature with an applied magnetic field of up to 3 T. (b) Temperature dependence of m_L/m_S ratio. Co hcp ratio value (0.08) is indicated by a black line and the calculated value for the low pressure sample by a blue line. (c) XMCD difference between spectrum recorded at 10 and 200 K. The resulting spectrum was multiplied by 2.4 for comparison with the 10 K spectrum of the sample grown at 10^{-4} mbar.

This observation is further supported by the temperature dependence of the Co $L_{2,3}$ edges XMCD spectra recorded on a 150 nm film grown at 10^{-6} mbar (figure 6(a)) indicative of a poorly ionic behavior. Furthermore, the fine structure progressively vanishes as the temperature increases to room temperature. This is not related to some structural changes since the shape of the XAS spectra, which are sensitive to all Co atoms, do not show any modifications. We can extract the m_L/m_S ratio considering the sum rules [16] for the dichroic signal. The evolution of the m_L/m_S ratio with the temperature is presented in figure 6(b). As the temperature is increased, the m_L/m_S ratio progressively decreases and tends at room temperature to a value corresponding to that of Co metal. Such a behavior could be attributed to the progressive decrease in temperature of Co^{2+} paramagnetic component to the magnetic signal. The measured signal at room temperature then predominantly arises from the superparamagnetic Co clusters. In figure 6(c), we show the difference between the XMCD spectrum at 10 K and the XMCD spectrum at 200 K. Doing this, we subtract the Co clusters contribution seen at high temperature to the spectrum recorded at 10 K. The resulting spectrum is quite close to the spectrum recorded at 10 K for the sample grown at higher oxygen pressure. This result points out unambiguously the presence of two Co phases in Co–LSTO films grown at low oxygen pressure. This is reminiscent of the presence of clusters reported recently by Zhang *et al* in 5% Co-doped (La, Sr)TiO_3 *et al* [10].

In summary, we have performed XAS and XMCD experiments at the Co $L_{2,3}$ edges of Co–LSTO samples. We report a very different behavior for samples grown at different oxygen pressures. The XAS and XMCD spectra of the sample grown at 10^{-4} mbar are typical of Co^{2+} at Ti sites, i.e. in an octahedral symmetry. The magnetic signal is characteristic of a paramagnetic behavior, which could be attributed to uncoupled Co^{2+} spins. The situation is more complex for the sample grown at 10^{-7} mbar. The XAS spectra unambiguously reveal the presence of Co^{2+} at Ti sites but the magnetic behavior observed by XMCD at low temperature as well as the temperature dependence of the m_L/m_S ratio are consistent with a superparamagnetic behavior related to the presence of metallic Co clusters, as recently found by HRTEM by others on 5% doped Co–LSTO [10]. Despite an intensive structural study including HRTEM and EELS on 2% doped Co–LSTO thin films [9] we were unable to identify such defects in our films. Therefore, the anisotropy observed with Co L_3 magnetometry measurements, possibly related to a ferromagnetic behavior, remains to be fully explained.

Acknowledgments

The authors thank Stéphane Fusil for fruitful discussions and valuable support and Patrick Berthet for preparing the PLD target.

References

[1] Chappert C, Fert A and Nguyen Van Dau F 2007 *Nat. Mater.* **6** 813
[2] Ohno H *et al* 1996 *Appl. Phys. Lett.* **69** 363
[3] Matsumoto Y *et al* 2001 *Science* **291** 854
[4] Dietl T *et al* 2000 *Science* **287** 1019
[5] Coey J M D 2006 *Curr. Opin. Solid State Mater. Sci.* **10** 83
[6] Rode K *et al* 2008 *Appl. Phys. Lett.* **92** 012509
[7] Zhao Y G *et al* 2003 *Appl. Phys. Lett.* **83** 2199
[8] Tokura Y *et al* 1993 *Phys. Rev. Lett.* **70** 2126
[9] Herranz G *et al* 2006 *Phys. Rev. Lett.* **96** 027207
[10] Zhang S X *et al* 2007 *Phys. Rev.* B **76** 085323
[11] Fujimori A *et al* 1992 *Phys. Rev.* B **46** 9841
[12] de Groot F M F *et al* 1989 *Phys. Rev.* B **40** 5715
[13] de Groot F M F *et al* 1990 *Phys. Rev.* B **42** 5459

[14] Imada S *et al* 1992 *J. Magn. Magn. Mater.* **104** 2001
[15] Escax V *et al* 2005 *Angew. Chem.* **117** 4876
[16] Chen C T *et al* 1995 *Phys. Rev. Lett.* **75** 152
[17] Cowan R D 1981 *The Theory of the Atomic Structure and Spectra* (Berkley: University of California Press)
Thole B T, Cowan R D, Sawatzky G A, Fink J and Fuggle J C 1985 *Phys. Rev.* B **31** 6856
[18] Higuchi T *et al* 1999 *Phys. Rev.* B **60** 7711
[19] Higuchi T *et al* 2003 *Phys. Rev.* B **68** 104420
[20] Hochepied J F *et al* 2001 *J. Magn. Magn. Mater.* **231** 315